scientific reports

Check for updates

OPEN

Photo-oscillations in MgZnO/ZnO heterostructures

Jesús Iñarrea

We theoretically examine the characteristics of microwave-induced magnetoresistance (MIRO) and photovoltage oscillations in MgZno/ZnO heterostructures. We demonstrate that both kind of oscillations, although described with different physical properties, are intimately related sharing the same physical origin. We use the radiation driven electron orbit model showing that the interplay of radiation driven swinging Landau orbits and the scattering processes are at the heart of the oscillations in both scenarios. Thus, our simulations show that all photo-oscillations present the main features of MIRO: they are periodic with the inverse of the magnetic field and the oscillations minima are 1/4 cycle shifted.

Microwave-induced resistance oscillations (MIRO)[1,2], envisaged by Ryzhii[3,66] in the 70's, are one of the most important effects when it comes to radiation-matter interaction in two dimensional electron systems (2DES). These peculiar oscillations present some distinctive features that serve to identified them. For instance, we can highlight, that they are periodic with the inverse of the magnetic field (B), the oscillations minima are shifted in 1/4 of the oscillation cycle and their amplitude exhibits a sublinear law with the power radiation (P) that at low power values gets linear. Closely related with the MIRO's power dependence there is another remarkable effect such as zero resistance states, (ZRS). They shows up when P is high enough[1]. Despite the fact that a lot of experimental[4–29,67] and theoretical[30–47] works have been carried out, the physical origin of MIRO and ZRS remain still unclear.

MIRO were discovered two decades ago in a high mobility GaAs/AlGaAs heterostructure when measuring irradiated magnetoresistance under a vertical magnetic field (B) at very low temperatures, $T \sim 1K$. Later on, similar oscillations were discovered when measuring another physical quantity such as photovoltage[48,50,51]. These novel oscillations presented the same peculiar features as MIRO did, suggesting similar, or at least related, physical origin[52,53]. MIRO have been observed in a bunch of different platforms, all of them holding a system of 2D carriers being irradiated from microwaves to terahertz under moderate B. These platforms include heterostructures such as, GaAs/AlGaAs[1,2], MgZnO/ZnO[54], GeSi/Ge[55] and more recently hexagonal boron nitride encapsulated graphene[56–59].

In this article, we present theoretical results on photo-oscillations of irradiated magnetoresistance (R_{xx}) and photovoltage using as platform the MgZnO/ZnO heterostructure[54]. This heterostructure is able to host a 2DES reaching a mobility about 1×10^6 cm^2/Vs with the improvements in the growth techniques[54,60]. This makes MgZnO/ZnO a good candidate to observe MIRO[54]. The goal of this work is to present a common microscopic theory explaining the radiation-induced oscillations experimentally observed in both R_{xx} and photovoltage. This theory stems from the previous model of *the radiation-driven electron orbits model*[30,31,43] which in turn is based on two main effects: the radiation-driven electron orbit motion and the corresponding scattering of electrons with impurities. According to our model the interplay of both effects would be at the heart of MIRO and photovoltage oscillations. Another important point that makes MgZnO/ZnO heterostructures very interesting and unique is that the source of scattering is different with respect to the most commonly used AlGaAs/GaAs platforms. In the latter case the main source of scattering is long-range potential centers such as remote charged impurities. However in the former, short-range potential scattering centers such as alloy impurities and surface roughness are the predominant contributors to disorder. In the present work, we have treated this kind of scattering with a model of a neutral impurity.

Theoretical model

The radiation-driven electron orbits model is a previously developed theoretical approach to explain both MIRO and ZRS that were observed in irradiated GaAsAl/GaAs heterostructures. One of the main results of this theory is that the Landau orbits are driven harmonically by radiation and the corresponding guiding center describes harmonic and classical trajectories on the 2D system. Accordingly, the interplay of this driven-harmonic motion

[1]Escuela Politécnica Superior, Universidad Carlos III, Leganes, 28911 Madrid, Spain. [2]Unidad Asociada al Instituto de Ciencia de Materiales, CSIC, Cantoblanco, 28049 Madrid, Spain. email: jinarrea@fis.uc3m.es

and scattering with sample disorder are at the core of photo-oscillations. Previous to irradiating the sample, electrons interact via scattering with the system disorder giving rise to resistance. In principle, the scattering is performed randomly in any direction leading to no net effect. Nevertheless, if there exists a DC electric field on the 2D sample, that can either be externally applied or built-in[48], a definite direction is determined that, on average, will be followed by the electron when interacting with scatterers. In each scattering jump the scattered electron advances an average distance, ΔX_0 along the DC field direction[49]. Thus, a certain current shows up that can be measured in terms of magnetoresistance R_{xx}[1,2] or photovoltage[48].

The scattering scenario in the dark is deeply altered when the sample is illuminated because the Landau orbits oscillate[30,31,43]. This novel situation can be experimentally observed via R_{xx}[1,2] or, more recently, via photovoltage[48,54]. Now, under radiation, the advanced distance or spatial shift, due to scattering, turns into a harmonic function according to the radiation-driven electron orbit model[30,31,43],

$$\Delta X = \Delta X_0 - A \sin\left(2\pi \frac{w}{w_c}\right) \tag{1}$$

where w and w_c are the radiation and cyclotron frequencies respectively and A is the oscillation amplitude,

$$A = \frac{e^{-\gamma\tau/2} e E_o}{m^* \sqrt{(w_c^2 - w^2)^2 + \gamma^4}} \tag{2}$$

where E_0 is the radiation electric field amplitude. According to Eq. (1), the radiation-driven Landau states, perform a swinging motion where the electrons interact with the lattice ions resulting in a damping process. The latter is phenomenologically introduced through the γ damping term[30,31,43].

If we now focus on the irradiated R_{xx}, we have to calculate first the corresponding conductivity σ_{xx} following a semiclassical Boltzmann approach[61–63],

$$\sigma_{xx} = 2e^2 \int_0^\infty dE \rho_i(E) (\Delta X)^2 W_I \left(-\frac{df(E)}{dE}\right) \tag{3}$$

being E the energy, $\rho_i(E)$ the density of initial Landau states and W_I is the scattering rate of electrons with sample disorder. According to the Fermi's golden rule: $W_I = N_i \frac{2\pi}{\hbar} | < \phi_f | V_r | \phi_i > |^2 \delta(E_i - E_f)$, where N_i is the number of impurities, ϕ_i and ϕ_f are the wave functions corresponding to the initial and final Landau states respectively and V_r is the disorder scattering potential. E_i and E_f stand for the initial and final energies. The V_r matrix element is given by[61,63]:

$$| < \phi_f | V_r | \phi_i > |^2 = \sum_q |V_q|^2 |I_{i,f}|^2 \tag{4}$$

and the term $I_{i,f}$[61,63],

$$I_{i,f} = \int \phi_f(x - X_0^{'}) exp(iq_x x) \phi_i(x - X_0) dx \tag{5}$$

where X_0 and $X_0^{'}$ are the guiding centers of the initial and final Landau states respectively and q_x the x-component of $\overrightarrow{q}$, the electron momentum change after the scattering event.

In the MgZno/ZnO system the main source of disorder and scattering is no longer long-range Coulomb potential centers such as remote charged impurities in AlGaAs/GaAs heterostructures. Now, short-range potential disorder is the main source of scattering. The heterointerface between MgZnO and ZnO takes in most of the disorder due to the Mg atoms that diffuse into the ZnO inversion layer. Thus, to calculate W_I we have considered a simple model of a 2D neutral impurity[64] (Mg atoms) based on a circular barrier of radius a. This constant potential is given by: $V_r = V_0$ if $r \leq a$ and $V_r = 0$ if $r > a$. Thus, V_0 plays the role of the scattering potential. In the calculation of W_I the Fourier transform $V(|\overrightarrow{q}|)$ of the potential V_r, needs to be obtained and accordingly is given by[64],

$$V(|\overrightarrow{q}|) = \pi a^2 V_0 \frac{2J_1(|\overrightarrow{q}|a)}{|\overrightarrow{q}|aS} \tag{6}$$

where J_1 is the first order Bessel function and S is the sample surface. Now we consider that $|\overrightarrow{q}|$ is small and thus $V(q)$ no longer depends on q and the scattering becomes isotropic. Then $V(|\overrightarrow{q}|)$ takes the form, $V(|\overrightarrow{q}|) \simeq \pi a^2 V_0 / S$. In our simulations we have used for a the effective Bhor radius[64] that in the case of ZnO is of the order of 2 nm. For V_0 we have used for a neutral impurity an estimate of[61,65] $V_0 \sim 50$ meV. Finally, R_{xx} is calculated according to the usual tensorial relations, $R_{xx} = \frac{\sigma_{xx}}{\sigma_{xx}^2 + \sigma_{xy}^2}$, where $\sigma_{xy} \simeq \frac{n_i e}{B}$, n_i being the electrons density, and e the electron charge. Then, and according to Eq. (3), the distance ΔX is direct responsible of the rise of MIRO when measuring R_{xx}.

The joint effect of radiation-driven Landau states and impurity scattering as origin of photo-oscillations can be revealed by measuring photovoltage instead of irradiated R_{xx}[59]. As we have indicated above, in order to obtain a net scattering we need a predominant direction along which the scattering jump takes place. This direction is determined by a DC electric field acting on the sample. In the case of R_{xx} this DC field is externally applied[1,2]. Nevertheless, in the case of photovoltage it can be either built-in[48] due, for instance to the presence in the sample

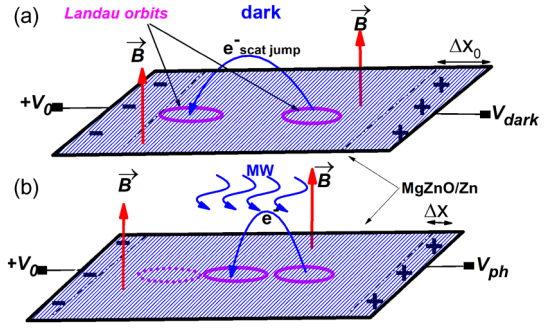

Figure 1. Schematic diagram of the microscopic model of dark voltage and photovoltage in MgZnO/ZnO heterostructures. The scattering direction is determined by the external voltage $+V_0$. (**a**) In the dark case the scattered electron mostly jump, between Landau orbits, in the direction of the positive voltage. As a result two lines of opposite charges build up at facing sides of the sample. (**b**) With radiation, the scattering jump distance changes due to the swinging motion of driven Landau orbits giving rise to radiation-induced photovoltage oscillations. The case of a shorter distance jump regarding the dark case is shown.

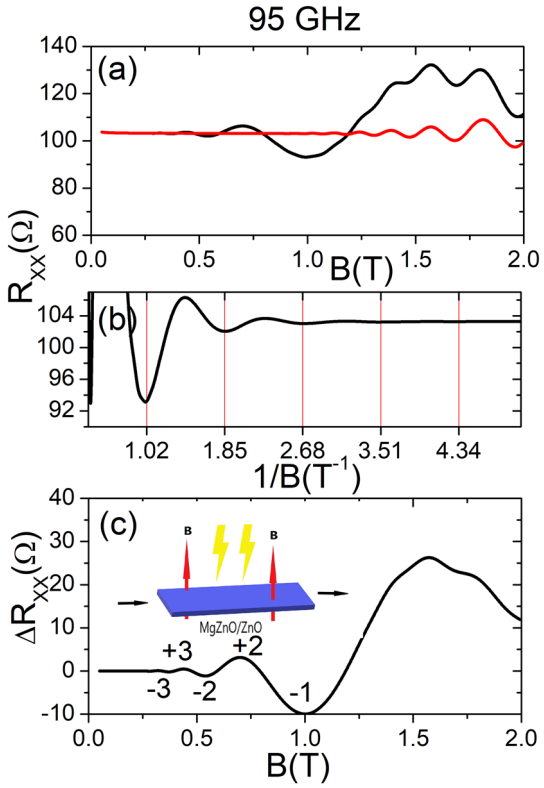

Figure 2. (**a**) Calculated irradiated (black curve) and dark (red curve) R_{xx} vs B. The radiation frequency is 95 GHz and $T = 1.0$ K. SdH oscillations are observed in both curves and in the irradiated one MIRO. (**b**) Irradiated R_{xx} vs the inverse of B. The corresponding curve is perfectly periodic. (**c**) Calculated MIRO amplitude ΔR_{xx} vs B. The labels in the figure correspond to the extrema positions (maxima and minima). The inset shows the basic experimental setup.

of metallic connection pads, or externally applied[56]. To theoretically study photovoltage in MgZno/ZnO systems we have applied a model previously used for encapsulated graphene[59]. In it, one of the squared sample edges is connected to an external positive DC voltage, $+V_0$ and then a definite scattering direction is determined in the sample (see Fig. 1). As a result two lines of opposite charge rise at facing sides. The lines width is of the order of the scattering spatial shift between Landau states[30,31,43] ΔX_0. Then, a voltage drop, V_{dark}, is created along the sample and can be experimentally measured. An expression for V_{dark} can be obtained, from basic electrostatics,

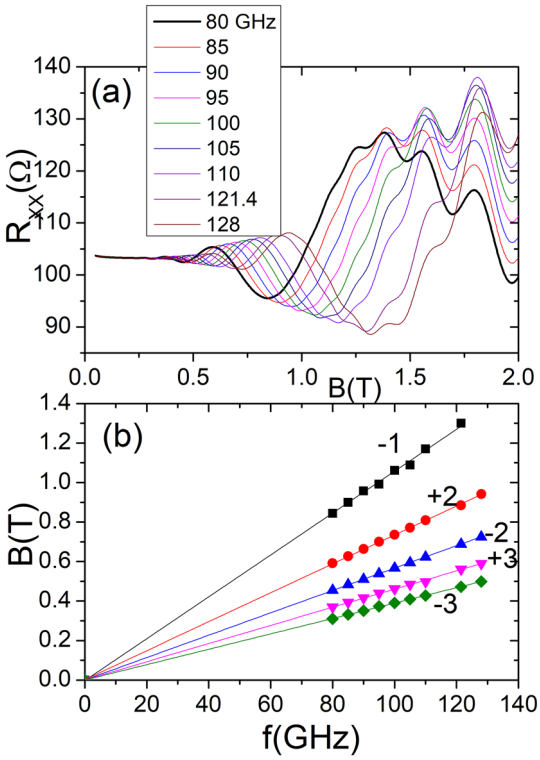

Figure 3. Frequency dependence of irradiated R_{xx} vs B. In the upper panel we exhibit irradiated R_{xx} vs B for nine different frequencies. Frequencies run from 80 to 128 GHz. Oscillations displace to higher B as frequency increases. In the lower panel the five groups of points correspond to the extrema positions labelled in Fig. 2. They show the dependence of extrema positions with B. The fits show that this dependence follow a straight line in all cases.

$$V_{dark} = \frac{n_{2D} e \Delta X_0}{2\pi\epsilon} \tag{7}$$

where e is the electron charge, ϵ is the ZnO permittivity and n_{2D} is the 2D charge density on the lines. n_{2D} can be expressed in function of the density of states per unit area around the Fermi energy $D(E_F)$, $n_{2D}(E_F) = 2D(E_F)\Delta E_F$, where ΔE_F is an energy interval around the Fermi energy. Thus, $D(E_F)$ accounts for the SdH oscillations that show up in the photovoltage. Under irradiation ΔX_0 turns into a harmonic function[44] $\Delta X = \Delta X_0 - A \sin\left(2\pi \frac{w}{w_c}\right)$ and instead of V_{dark} there is a photovoltage, V_{ph} given by an expression similar to V_{dark} but with ΔX instead of ΔX_0.

Results

In Fig. 2 upper panel we exhibit two curves of R_{xx} vs B for MgZnO/ZnO. The black curve corresponds to irradiated R_{xx} and the red curve to the dark case. The radiation frequency is 95 GHz and $T = 1.0$ K. In both curves we can observe SdH oscillations and in the irradiated also MIRO, as occurs in other semiconductor platforms. The main photo-oscillations shows up at higher B regarding AlGaAs/GaAs due to the bigger effective mass. In our simulations for MgZnO/ZnO we have used $m^* = 0.35m_e$ where m_e is the bare electron mass[54]. In contrast, for AlGaAs/GaAs the usual effective is around $m^* = 0.067m_e$ and the oscillations show up at smaller B. For the electron density we have used $n_e = 5 \times 10^{11}$ cm^{-2} and a mobility of 1×10^5 cm^2/Vs. These are similar values as the ones of the experiments[54]. In the middle panel we represent irradiated R_{xx} vs the inverse of B. The corresponding curve is perfectly periodic, as expected fulfilling one of the distinctive MIRO features. The vertical lines at the minima positions act as a help to check the oscillations periodicity with $1/B$. In the lower one we exhibit the oscillations amplitude ΔR_{xx} vs B, so that he extrema positions can be more easily identified. The labels in the figure correspond to the extrema (maxima and minima). The oscillations minima show the shift of 1/4 in the oscillation cycle, which is another peculiar MIRO feature. Thus, their position varies as $w/w_c = 1/4 + j$, j being a positive integer. The inset shows the basic experimental setup. The calculated results are in qualitatively agreement with experiment[54].

In Fig. 3 we plot the radiation frequency dependence of irradiated magnetoresistance in MgZnO/ZnO. In the upper panel we present irradiated R_{xx} vs B for nine different frequencies from 80 to 128 GHz. All the curves are 1/4 cycle shifted irrespective of the frequency. We observe that MIRO displace to higher B as frequency increases, increasing as well the number of oscillations. The extrema change their positions in the B axis according to a

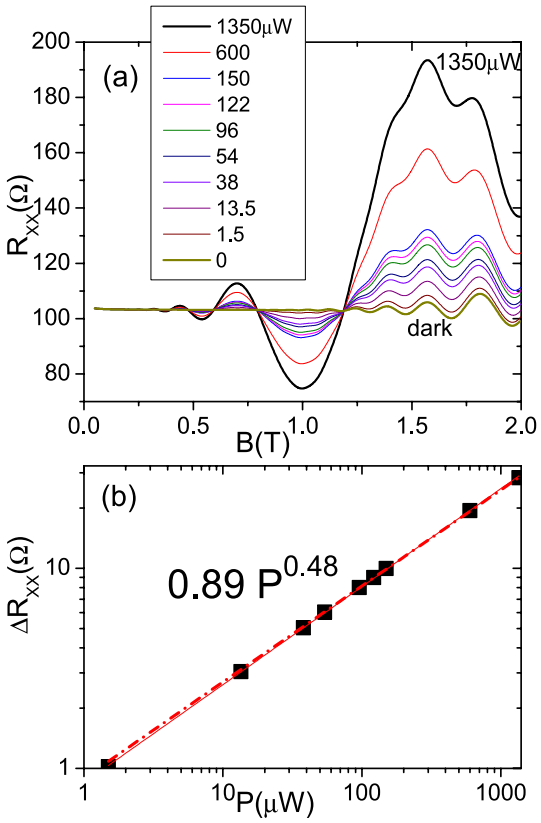

Figure 4. In the upper panel we present the radiation power dependence of irradiated R_{xx} vs B. Ten curves are exhibited corresponding to ten different power values ranging from the dark case to 1350 μW. As P rises the oscillations amplitude increases too. On the other hand P does not alter the oscillations position that keep constant as P increases. In the lower panel we presene the irradiated R_{xx} amplitude vs P. $T = 1$ K.

definite dependence; for the minima according to $w/w_c = 1/4 + j, j$ and for the maxima, $w/w_c = 3/4 + j, j$. This dependence is revealed in the lower panel where we represent B versus radiation frequency for five cases corresponding to the extrema labelled in Fig. 2 lower panel. We have carried out fits on every group of points obtaining very clear straight lines, as expected according to the two previous formula that relate w and w_c. The variation of extrema positions with B according to a straight line is another genuine characteristic of MIRO and has been experimentally observed in previous semiconductor platforms. Again the calculated results are in qualitatively good agreement with the experimental ones[54].

Figure 4 shows the power dependence of irradiated magnetoresistance in MgZnO/ZnO. In the upper panel we present irradiated R_{xx} vs B for ten different power values ranging from 0 to 1350 μW. As the power increases the MIRO amplitude rises too following a square root law: $\Delta R_{xx} \propto P^{0.5}$. The P increase does not affect the oscillations position that keep constant. The power Law dependence is exhibited in the lower panel where we present ΔR_{xx} amplitude vs P. We fit the calculated points obtaining a square root dependence (dashed red curve) of ΔR_{xx} with P: $\Delta R_{xx} = 0.89P^{0.48}$. Despite the controversy between linear and square root dependence, we have to admit that a good number of experiments show a mixed behaviour between linear and sublinear. The most recent experiments with encapsulated monolayer graphene[56], show a linear dependence at low power and as the latter increases, the dependence becomes sublinear.

We now focus on the photovoltage results. Thus, in the upper panel of Fig. 5 we exhibit photovoltage vs B for a frequency of 95 GHz and $T = 1$ K. The curve is qualitatively very similar to the one of irradiated R_{xx} in Fig. 2a. In the middle panel we exhibit photovoltage amplitude vs B. Both curves in (a) and (b) present the main characteristics of MIRO that were already obtained when calculating magnetoresistance: photovoltage turns out to be periodic with $1/B$ (not shown in the figure) and minima positions are 1/4 cycle shifted. The extrema positions coincide with the ones obtained in irradiated R_{xx}. Finally in the lower one we observe that photovoltage follows a square root law when it comes to radiation power dependence.

Conclusions

Summing up, we have theoretically studied the microwave-induced resistance oscillations and photo oscillations experimentally found in MgZnO/ZnO heterostructures. We have used the radiation-driven electron orbit model to depict a common microscopic model for both kind of oscillations. We have come to the conclusion that the interplay between the radiation-driven Landau orbits that perform harmonic trajectories and the interaction with

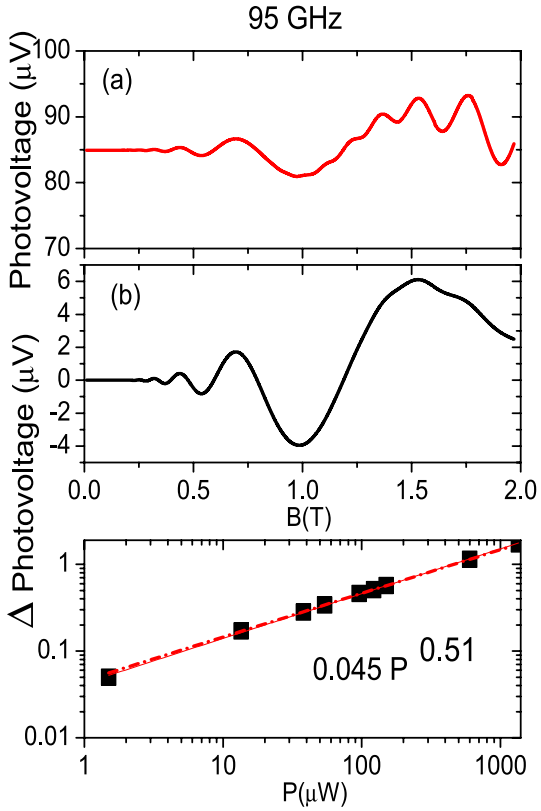

Figure 5. Frequency dependence of the calculated photovoltage vs B, showing four frequencies in the THz range: 0.7, 1, 1.5 and 2.0 THz. As the frequency rises the number of oscillations increases but the oscillations amplitude lowers. $T = 1$ K.

the sample disorder are at the origin of both photo-oscillations. Thus both show the main distinctive characteristics of previous MIRO. They are periodic with the inverse of the magnetic field and they are 1/4 cycle shifted. The calculated results both, magnetoresitance and photovoltage are in qualitative good agreement with experiments[54] except in the part of power dependence where experiments shows a linear behavior at low radiation power.

Data availability

All data generated or analysed during this study are included in this published article.

Received: 28 September 2022; Accepted: 26 December 2022
Published online: 28 December 2022

References

1. Mani, R. . G. *et al.* Zero-resistance states induced by electromagnetic-wave excitation in GaAs/AlGaAs heterostructures. *Nature (London)* **420**, 646 (2002).
2. Zudov, M. A., Du, R. R., Pfeiffer, L. N. & West, K. W. Evidence for a new dissipationless effect in 2D electronic transport. *Phys. Rev. Lett.* **90**, 046807 (2003).
3. Ryzhii, V. I. Photoconductivity characteristics in thin films subjected to crossed electric and magnetic fields. *Sov. Phys. Solid State* **11**, 2078 (1970).
4. Mani, R. G. *et al.* Demonstration of a 1/4-cycle phase shift in the radiation-induced oscillatory magnetoresistance in GaAs/AlGaAs devices. *Phys. Rev. Lett.* **92**, 146801 (2004).
5. Mani, R. G. *et al.* Radiation-induced oscillatory magnetoresistance as a sensitive probe of the zero-field spin-splitting in high-mobility GaAs/AlxGa1-xAs devices. *Phys. Rev. B* **69**, 193304 (2004).
6. Willett, R. L., Pfeiffer, L. N. & West, K. W. Evidence for current-flow anomalies in the irradiated 2D electron system at small magnetic fields. *Phys. Rev. Lett.* **93**, 026804 (2004).
7. Mani, R. G. Zero-resistance states induced by electromagnetic-wave excitation in GaAs/AlGaAs Heterostructures. *Phys. E* **22**, 1 (2004).
8. Smet, J. H. *et al.* Circular-polarization-dependent study of the microwave photoconductivity in a two-dimensional electron system. *Phys. Rev. Lett.* **95**, 116804 (2005).
9. Yuan, Z. Q., Yang, C. L., Du, R. R., Pfeiffer, L. N. & West, K. W. Microwave photoresistance of a high-mobility two-dimensional electron gas in a triangular antidot lattice. *Phys. Rev. B* **74**, 075313 (2006).
10. Mani, R. G., Johnson, W. B., Umansky, V., Narayanamurti, V. & Ploog, K. Phase study of oscillatory resistances in microwave-irradiated- and dark-GaAs/AlGaAs devices: Indications of an unfamiliar class of the integral quantum Hall effect. *Phys. Rev. B* **79**, 205320 (2009).

11. Wiedmann, S., Gusev, G. M., Raichev, O. E., Bakarov, A. K. & Portal, J. C. Microwave zero-resistance states in a bilayer electron system. *Phys. Rev. Lett.* **105**, 026804 (2010).
12. Wiedmann, S., Gusev, G. M., Raichev, O. E., Bakarov, A. K. & Portal, J. C. Crossover between distinct mechanisms of microwave photoresistance in bilayer systems. *Phys. Rev. B* **81**, 085311 (2010).
13. Konstantinov, D. & Kono, K. Novel radiation-induced magnetoresistance oscillations in a nondegenerate two-dimensional electron system on liquid helium. *Phys. Rev. Lett.* **103**, 266808 (2009).
14. Dorozhkin, S. . I., Pfeiffer, L., West, K., von Klitzing, K. K. & Smet, J. .H. Random telegraph photosignals in a microwave-exposed two-dimensional electron system. *Nat. Phys.* **7**, 336–341 (2011).
15. Mani, R. G., Gerl, C., Schmult, S., Wegscheider, W. & Umansky, V. Nonlinear growth in the amplitude of radiation-induced magnetoresistance oscillations. *Phys. Rev. B* **81**, 125320 (2010).
16. Mani, R. G., Ramanayaka, A. N. & Wegscheider, W. Observation of linear-polarization-sensitivity in the microwave-radiation-induced magnetoresistance oscillations. *Phys. Rev. B* **84**, 085308 (2011).
17. Inarrea, Jesus, Mani, R. .G. & Wegscheider, W. Sublinear radiation power dependence of photoexcited resistance oscillations in two-dimensional electron systems. *Phys. Rev.* **82**, 205321 (2010).
18. Mani, R. G. Photo-excited zero-resistance states in the gaas/algaas system. *Int. J. Mod. Phys. B* **18**, 3473 (2004).
19. Ye, Tianyu, Liu, Han-Chun., Wegscheider, W. & Mani, R. .G. Combined study of microwave-power/linear-polarization dependence of the microwave-radiation-induced magnetoresistance oscillations in GaAs/AlGaAs devices. *Phys. Rev. B* **89**, 155307 (2014).
20. Ye, T. Y., Liu, H. C., Wang, Z., Wegscheider, W. & Mani, R. G. Comparative study of microwave radiation-induced magnetoresistive oscillations induced by circularly- and linearly- polarized photo-excitation. *Sci. Rep.* **5**, 14880 (2015).
21. Savchenko, M. L. *et al.* Demonstration of high sensitivity of microwave-induced resistance oscillations to circular polarization. *Phys. Rev. B* **106**, L161408 (2022).
22. Otteneder, M. *et al.* Sign-alternating photoconductivity and magnetoresistance oscillations induced by terahertz radiation in HgTe quantum wells. *Phys. Rev. B* **98**, 245304 (2018).
23. Savchenko, M. L. *et al.* Terahertz photoresistivity of a high-mobility 3D topological insulator based on a strained HgTe film. *Appl. Phys. Lett.* **117**, 201103 (2020).
24. Dmitriev, I. A., Mirlin, A. D. & Polyakov, D. G. Cyclotron resonance harmonics in the ac response of a 2D electron gas with smooth disorder. *Phys. Rev. Lett.* **91**, 226802 (2003).
25. Dmitriev, I. A., Vavilov, M. G., Aleiner, I. L., Mirlin, A. D. & Polyakov, D. G. Theory of microwave-induced oscillations in the magnetoconductivity of a two-dimensional electron gas. *Phys. Rev. B* **71**, 115316 (2005).
26. Raichev, O. E. Magnetic oscillations of resistivity and absorption of radiation in quantum wells with two populated subbands. *Phys. Rev. B* **78**, 125304 (2008).
27. Dmitriev, I. A., Khodas, M., Mirlin, A. D., Polyakov, D. G. & Vavilov, M. G. Mechanisms of the microwave photoconductivity in two-dimensional electron systems with mixed disorder. *Phys. Rev. B* **80**, 165327 (2009).
28. Mikhailov, S. A. Theory of microwave-induced zero-resistance states in two-dimensional electron systems. *Phys. Rev. B* **83**, 155303 (2011).
29. Dmitriev, I. A., Mirlin, A. D., Polyakov, D. G. & Zudov, M. A. Nonequilibrium phenomena in high Landau levels. *Rev. Mod. Phys.* **84**, 1709 (2012).
30. Iñarrea, J. & Platero, G. Theoretical approach to microwave-radiation-induced zero-resistance states in 2D electron systems. *Phys. Rev. Lett.* **94**, 016806 (2005).
31. Iñarrea, J. & Platero, G. Temperature effects on microwave-induced resistivity oscillations and zero-resistance states in two-dimensional electron systems. *Phys. Rev. B* **72**, 193414 (2005).
32. Iñarrea, Jesus. Influence of linearly polarized radiation on magnetoresistance in irradiated two-dimensional electron systems. *Appl. Phys. Lett.* **100**, 242103 (2012).
33. Inarrea, J. & Platero, G. Microwave-induced resistance oscillations and zero-resistance states in two-dimensional electron systems with two occupied subbands. *Phys. Rev. B* **84**, 075313 (2011).
34. Iñarrea, Jesus. The two dimensional electron system as a nanoantenna in the microwave and terahertz bands. *Appl. Phys. Lett.* **99**, 232115 (2011).
35. Durst, A. C., Sachdev, S., Read, N. & Girvin, S. M. Radiation-induced magnetoresistance oscillations in a 2D electron gas. *Phys. Rev. Lett.* **91**, 086803 (2003).
36. Lei, X. L. & Liu, S. Y. Radiation-induced magnetoresistance oscillation in a two-dimensional electron gas in Faraday geometry. *Phys. Rev. Lett.* **91**, 226805 (2003).
37. Rivera, P. H. & Schulz, P. A. Radiation-induced zero-resistance states: Possible dressed electronic structure effects. *Phys. Rev. B* **70**, 075314 (2004).
38. Iñarrea, J. & Platero, G. Effect of an in-plane magnetic field on microwave-assisted magnetotransport in a two-dimensional electron system. *Phys. Rev. B* **78**, 193310 (2008).
39. Iñarrea, J. Effect of frequency and temperature on microwave-induced magnetoresistance oscillations in two-dimensional electron systems. *Appl. Phys. Lett.* **92**, 192113 (2008).
40. Inarrea, Jesus & Platero, Gloria. Microwave magnetoabsorption in two-dimensional electron systems. *Appl. Phys. Lett.* **95**, 162106 (2009).
41. Iñarrea, J. Anharmonic behavior in microwave-driven resistivity oscillations in Hall bars. *Appl. Phys. Lett.* **90**, 262101 (2007).
42. Inarrea, Jesus. Linear polarization sensitivity of magnetotransport in irradiated two-dimensional electron systems. *J. Appl. Phys.* **113**, 183717 (2013).
43. Inarrea, Jesus. Radiation-induced resistance oscillations in 2D electron systems with strong Rashba coupling. *Sci. Rep.* **7**, 13573 (2017).
44. Inarrea, Jesus & Platero, Gloria. Radiation-induced resistance oscillations in a 2D hole gas: A demonstration of a universal effect. *J. Phys. Condens. Matter* **27**, 415801 (2015).
45. Inarrea, J. & Platero, G. Driving Weiss oscillations to zero resistance states by microwave Radiation. *Appl. Phys. Lett.* **93**, 062104 (2008).
46. Iñarrea, Jesus & Platero, Gloria. Light-assisted magnetotunneling through a semiconductor double-barrier structure. *Phys. Rev. B* **51**, 5244 (1995).
47. Beltukov, Y. M. & Dyakonov, M. I. Microwave-induced resistance oscillations as a classical memory effect. *Phys. Rev. Lett.* **116**, 176801 (2016).
48. Dorozhkin, S. I. *et al. Phys. Rev. Lett.* **102**, 036602 (2009).
49. Savchenko, M. L. *et al.* High harmonics of the cyclotron resonance in microwave transmission of a high-mobility two-dimensional electron system. *Phys. Rev. Res.* **3**, L012013 (2021).
50. Bykov, A. A. *JETP Lett.* **87**, 233 (2008).
51. Mani, R. .G. *et al.* Terahertz photovoltaic detection of cyclotron resonance in the regime of radiation-induced magnetoresistance oscillations. *Phys. Rev. B* **87**, 245308 (2013).
52. Dmitriev, I. A., Dorozhkin, S. I. & Mirlin, A. D. Theory of microwave-induced photocurrent and photovoltage magneto-oscillations in a spatially nonuniform two-dimensional electron gas. *Phys. Rev. B* **80**, 125418 (2009).

53. Dmitriev, I. A., Dorozhkin, S. I. & Mirlin, A. D. Photogalvanic effects originating from the violation of the Einstein relation in a 2D electron gas in high Landau levels. *Physica E* **42**, 1159 (2010).
54. Kärcher, D. F. *et al.* and. *J. H. Smet Phys. Rev. B* **93**, 041410(R) (2016).
55. Zudov, M. A., Mironov, O. A., Ebner, Q. A., Martin, P. D. & Shi, Q. and D. *R. Leadley Phys. Rev. B* **89**, 125401 (2014).
56. Mönch, E. *et al. Nano Lett.* **20**, 5943 (2020).
57. Mani, R. G., Kriisa, A. & Munasinghe, R. *Sci. Rep.* **9**, 7278 (2019).
58. Iñarrea, Jesus & Platero, Gloria. *New J. Phys.* **23**, 063004 (2021).
59. Iñarrea, Jesus & Platero, Gloria. *Sci. Rep.* **12**, 5157 (2022).
60. Falson, Joseph *et al. Sci. Rep.* **6**, 26598 (2016).
61. Ridley, B. K. *Quantum Processes in Semiconductors* 4th edn. (Oxford University Press, Oxford, 1993).
62. Ando, T., Fowler, A. & Stern, F. *Rev. Mod. Phys.* **54** (1982).
63. Askerov, B. M. *Electron transport phenomena in semiconductors* (World Scientific, Singapore, 1994).
64. John, H. *Davies* (Cambridge University Press, The Physics of Low-dimensional Semiconductors, 1998).
65. El-Ghanem, H. M. A. & Ridley, B. K. *J. Phys. C: Solid St. Phys.* **13**, 2041 (1980).
66. Ryzhii, V. I., Suris, R. A. & Shchamkhalova, B. S. Photoconductivity of a two-dimensional electron-gas in a strong magnetic-field. *Sov. Phys. Semicond.* **20**, 1299 (1986).
67. Novel zero-resistance states induced by photoexcitation in the high mobility GaAs/AlGaAs two-dimensional electron system. *Phys. E* **25**, 189 (2004).

Acknowledgements

This work is supported by the MINECO (Spain) under grant PID2020-117787GB-I00 and by the Madrid Government (Comunidad de Madrid- Spain) under the Multiannual Agreement with UC3M in the line of Excellence of University Professors (EPUC3M14), and in the context of the V PRICIT (Regional Programme of Research and Technological Innovation). We also acknowledge the CSIC Research Platform on Quantum Technologies PTI-001.

Competing interests

The author declares no competing interests.

Additional information

Correspondence and requests for materials should be addressed to J.I.

Reprints and permissions information is available at www.nature.com/reprints.

Publisher's note Springer Nature remains neutral with regard to jurisdictional claims in published maps and institutional affiliations.